Sharing Geoscience Online
#shareEGU20
EGU2020-4174

A unified numerical model for the simulation of the seismic cycle for normal and reverse fault earthquakes in Italy

Matteo Albano[1] (matteo.albano@ingv.it; @matteo_albano), Salvatore Barba[1], Christian Bignami[1], Eugenio Carminati[2], Carlo Doglioni[1,2], Marco Moro[1], Michele Saroli[3], Salvatore Stramondo[1], Sergey Samsonov[4]

1 - Istituto Nazionale di Geofisica e Vulcanologia, Roma, Italy; 2 - "Sapienza" Università di Roma, Roma, Italy; 3 - Università degli Studi di Cassino e del Lazio Meridionale, Cassino, Italy; 4 – Natural Resources Canada, Ottawa, Canada

CONTEXT

- The dynamics of the preparation, initiation, occurrence, and evolution of earthquakes (i.e., the seismic cycle) are governed by several physical mechanisms and parameters that are often unknown.
- Understanding those mechanisms is crucial for developing new techniques and approaches for earthquake monitoring and hazard assessment.
- We contribute to the existing knowledge of the seismic cycle dynamics of a single fault plane by developing a first-order numerical model capable of jointly simulating quasi-static crustal interseismic loading, coseismic brittle episodic dislocations, and postseismic relaxation for extensional and compressional earthquakes in Italy.
- We simulated the interseismic, coseismic and postseismic phases of two seismic events in Italy; the 6 April 2009, M_w 6.1 L'Aquila normal fault earthquake and the 20 May 2012, M_w 5.9 Emilia reverse fault earthquake.

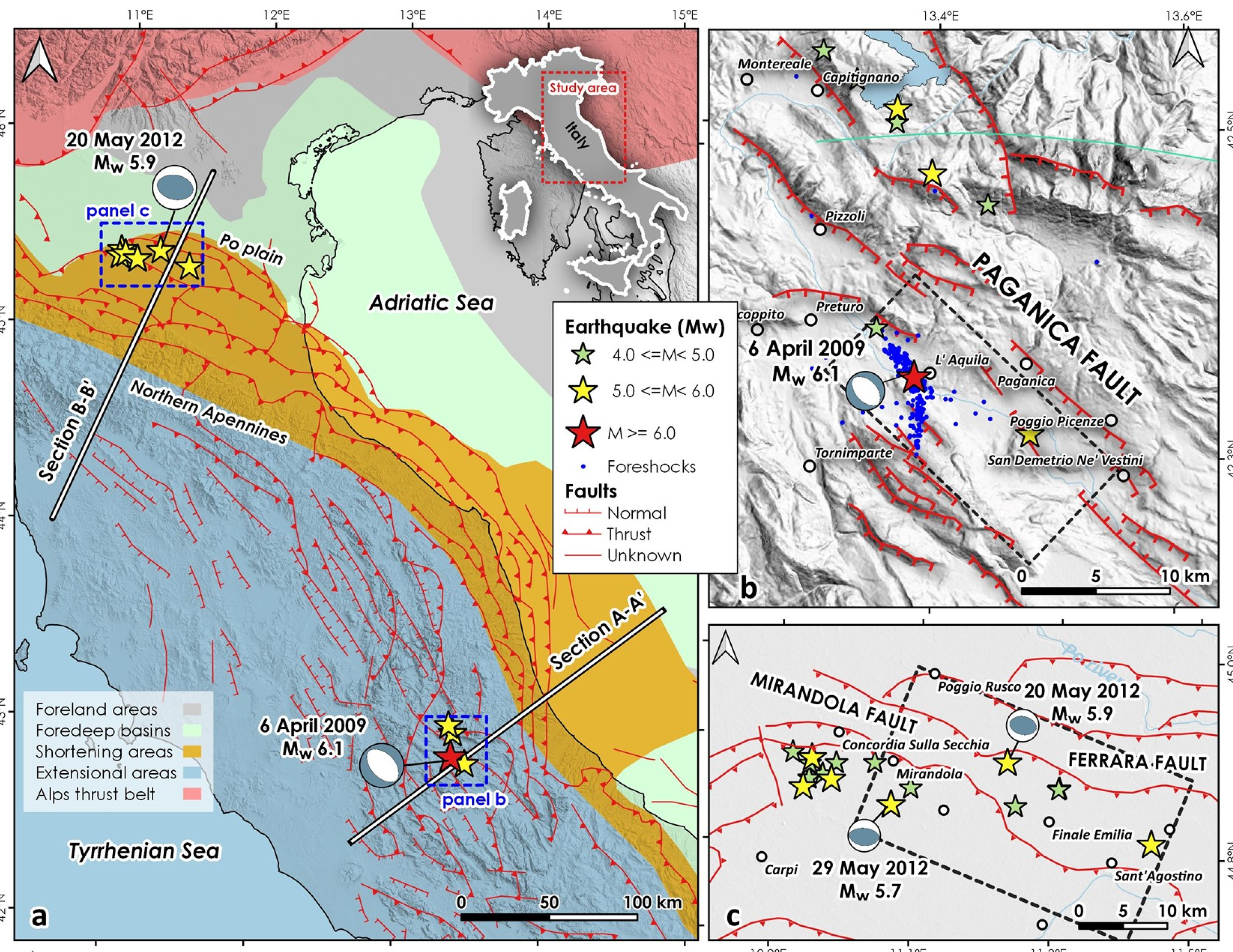

Fig. 1. Tectonic sketch of the study area. a) Simplified tectonic map showing the major tectonic and geodynamic setting of the region (modified from Carminati & Doglioni 2012), with the locations of the studied earthquakes and the footprints of panels b, and c. b) The L'Aquila 2009 seismic sequence. c) The Emilia 2012 seismic sequence. The black rectangles in panels b, and c indicate the projection at the surface of the fault planes responsible for the two events estimated from an analytical inversion of geodetic data.

Numerical model

- **Section A-A' (Figure 1a): L'Aquila 2009 earthquake model**

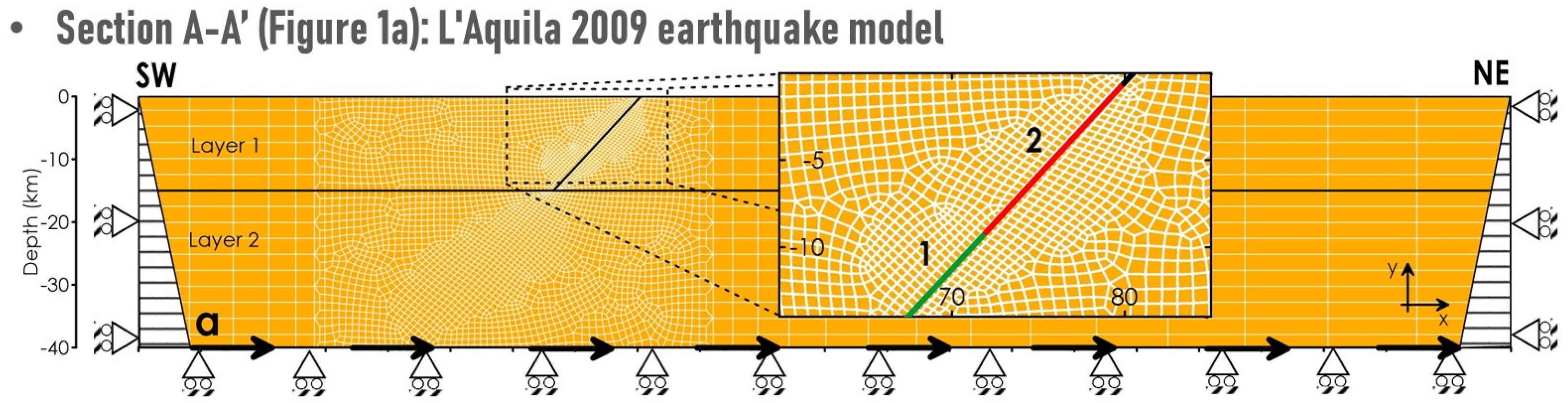

- **Section B-B' (Figure 1a): Emilia 2012 earthquake model**

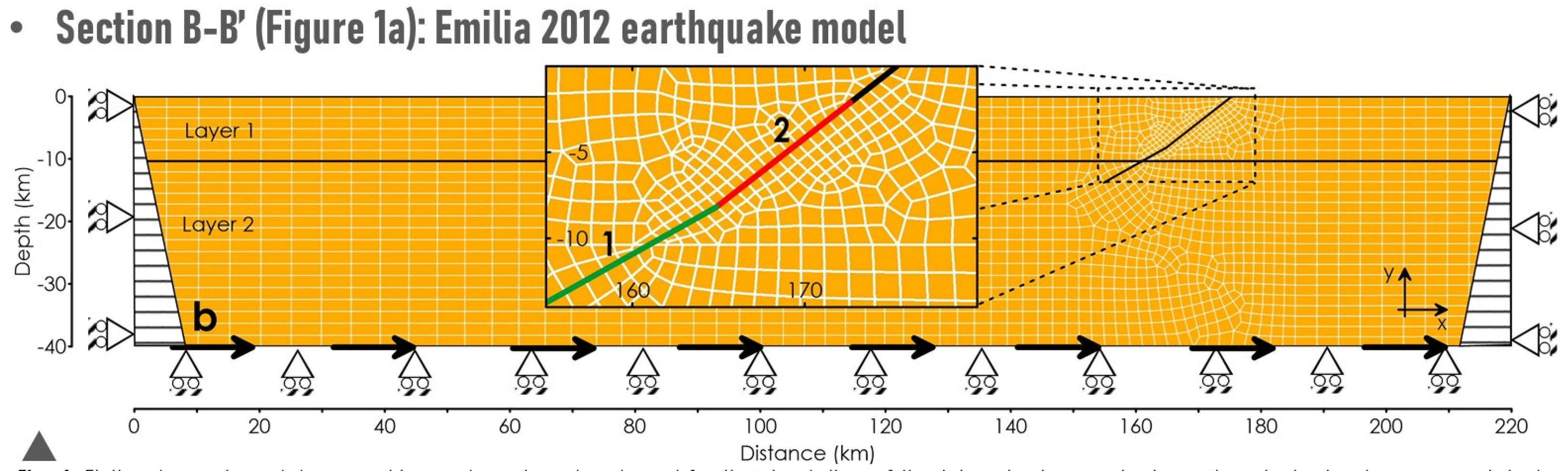

Fig. 4. Finite element model geometries and meshes developed for the simulation of the interseismic, coseismic and postseismic phases associated with the L'Aquila 2009 (a), and Emilia 2012 (b) earthquakes.

MATERIALS & METHODS

InSAR data

- **L'Aquila 2009 earthquake InSAR coseismic ground displacements**

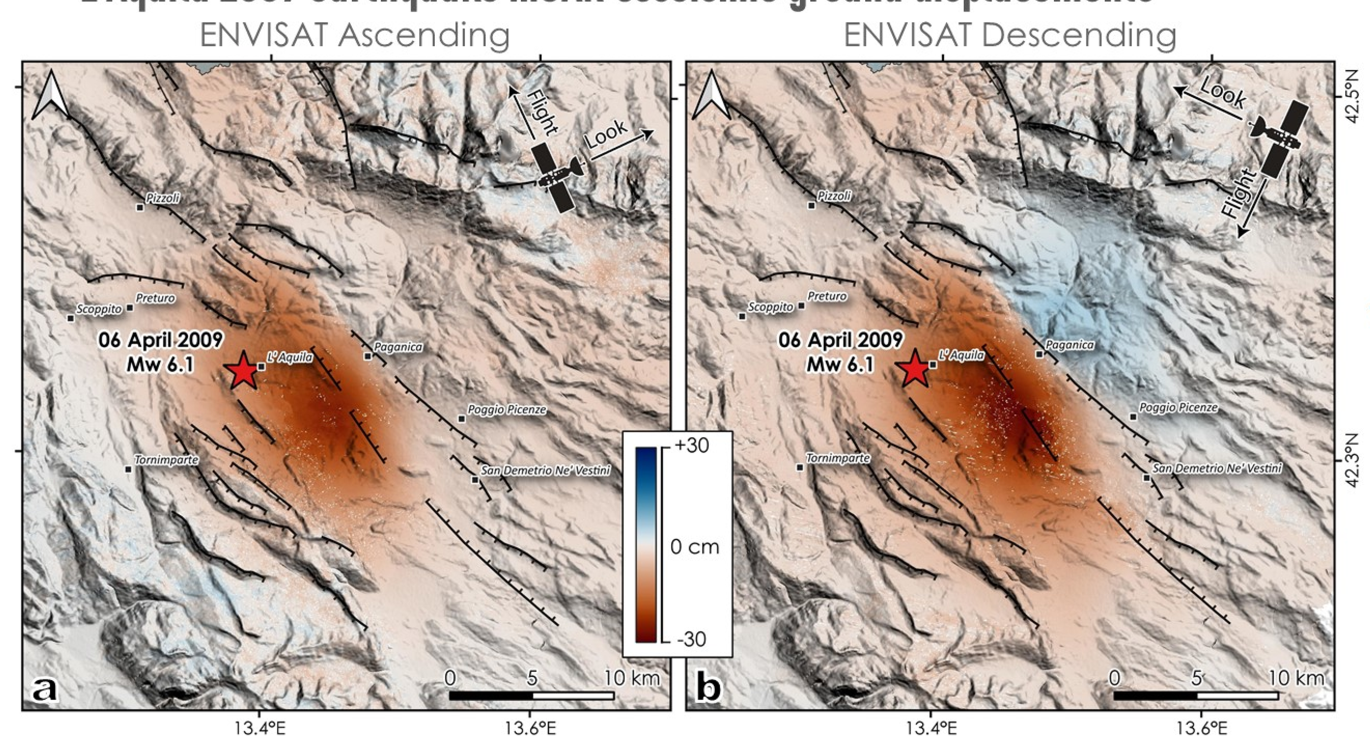

- **Emilia 2012 earthquake InSAR coseismic ground displacements**

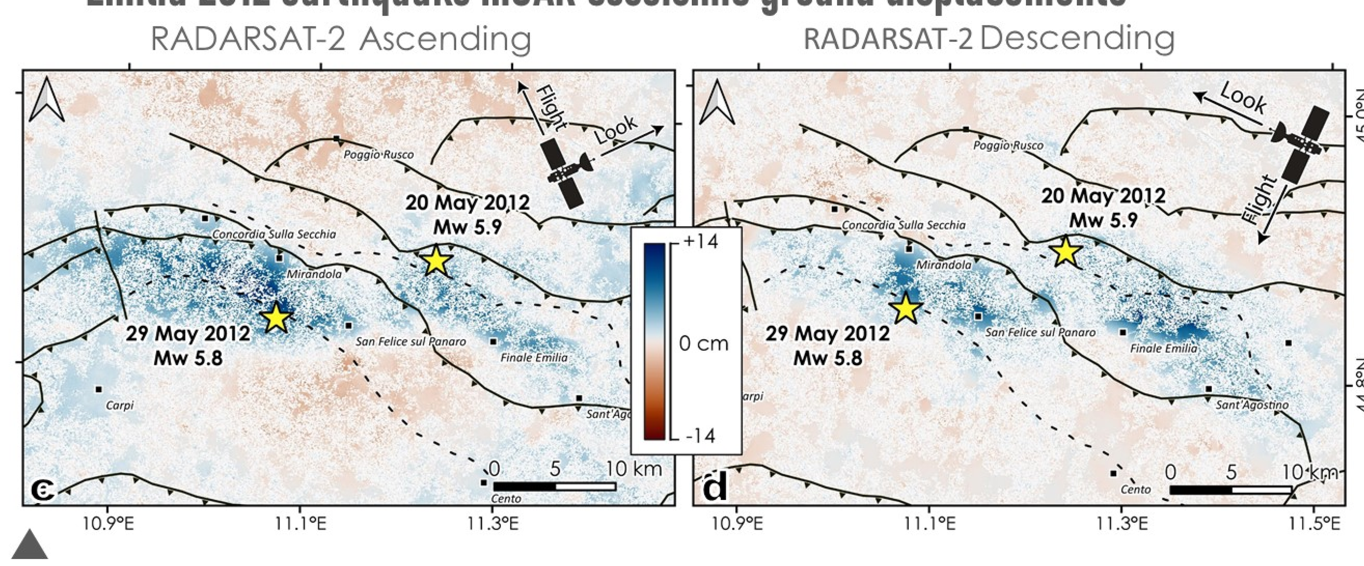

Fig. 2. Coseismic ground displacements from InSAR data. a) Ascending and b) descending LOS ground displacements associated with the M_w 6.1 L'Aquila 2009 event. c) Ascending and d) descending LOS ground displacements associated with the M_w 5.9 Emilia 2012 event.

Conceptual sketch

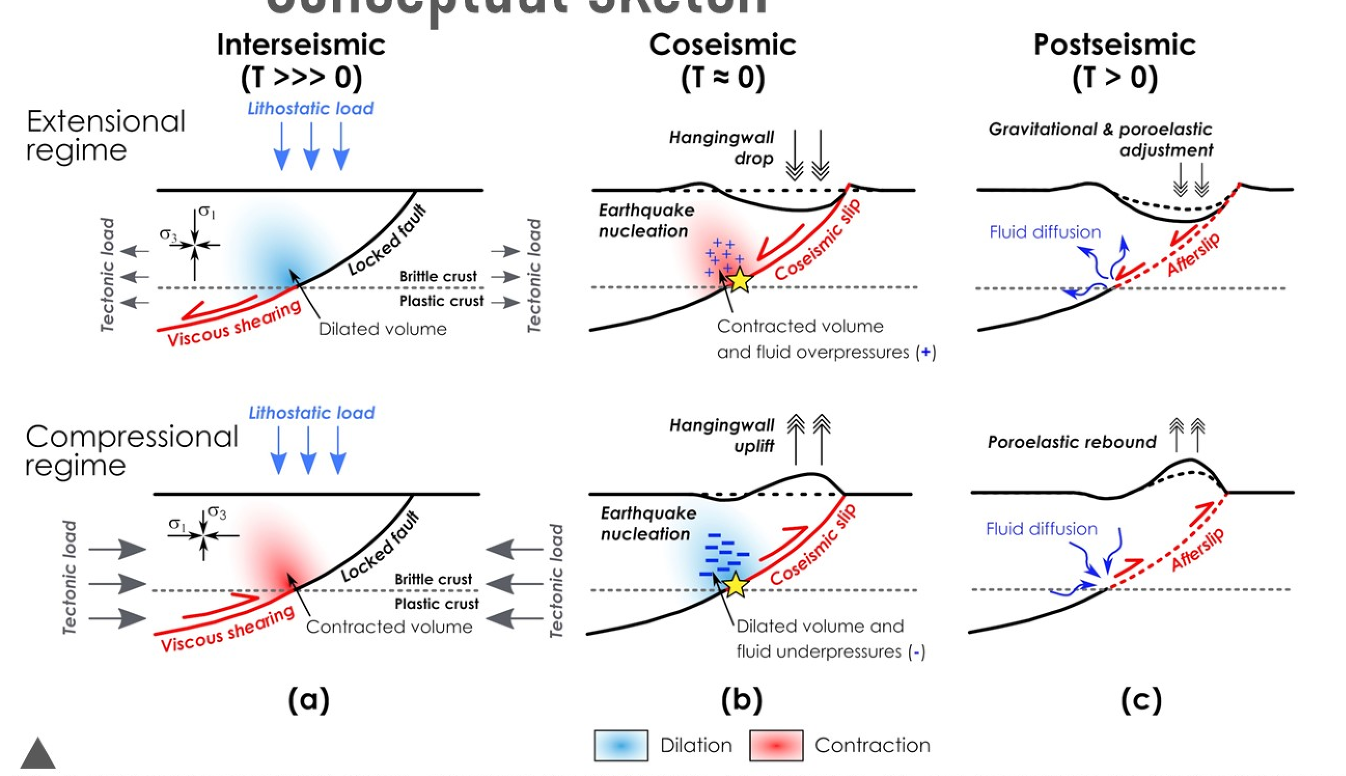

Fig. 3. First-order conceptual sketch explaining the interseismic (a) coseismic (b) and postseismic (c) phases for normal faulting (upper panels) and reverse faulting (lower panels) earthquakes (modified from Doglioni et al. 2011).

- Same boundary conditions and loads for normal and reverse fault mechanisms.
- The model is poroelastic and it is subjected to the lithostatic load and the tectonic load. The latter is modelled as a NE-oriented shear force applied at the model's base (black arrows in Fig. 4).
- Fault segments (1 and 2 in Fig. 4) are assumed locked or unlocked according to the modelled phase.
- Fault Kinematics (faulting style and amplitude) is governed by the applied boundary conditions and loads (no forces or displacements are applied along the fault's edges).
- Three modelling phases: 1) interseismic phase; 2) Coseismic phase; 3) Postseismic phase.

RESULTS

Intersesimic phase

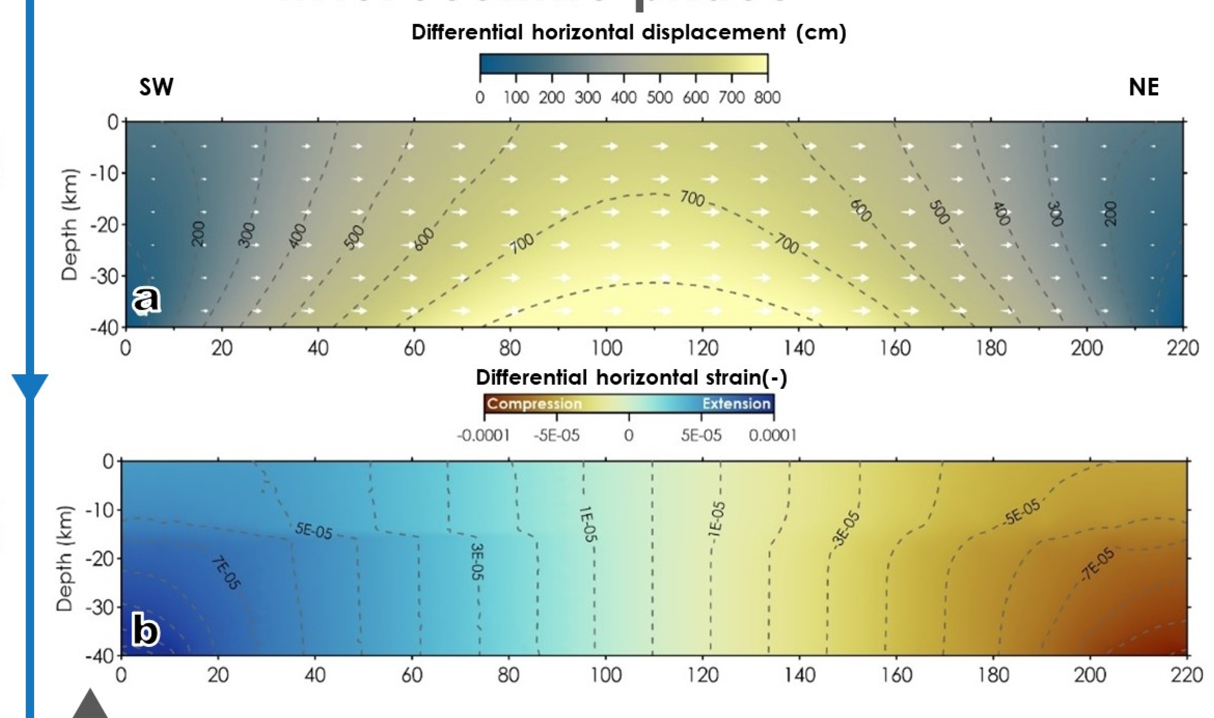

Fig. 5. The applied shear load at the model's base produces the interseismic horizontal displacement pattern in panel (a). As a result, the SW part of the model, corresponding to the Apennines Chain (Fig. 1a), is extended (panel b) while the NE part, corresponding to the Po plain and the Adriatic foreland (Fig. 1a) of the model is compressed. The L'Aquila 2009 and the Emilia 2012 fault segments (Fig. 4) are then subjected to an extensional and compressional tectonic stress field, respectively.

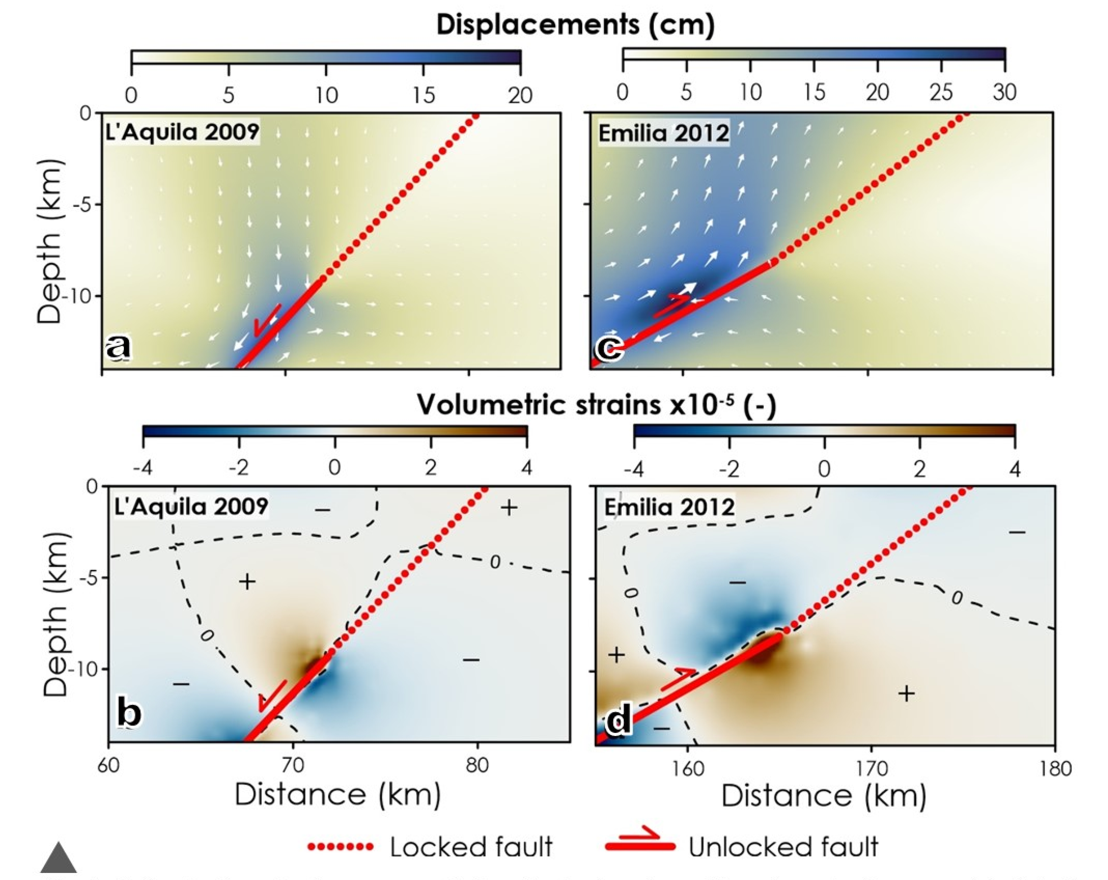

Fig. 6 At the fault scale, the assumed interseismic shearing of the deep fault segment (n°1 in Fig. 4) locally modifies the displacements stress and strains at the transition between the locked and unlocked segments. For the L'Aquila 2009 event, the normal fault dislocation (panel a) produces an increase of volumetric strains that indicate volume dilation (panel b). For the Emilia 2012 event, the reverse fault slip (panel c) causes a decrease of volumetric strains (panel d) that indicate volume contraction.

Coseismic phase

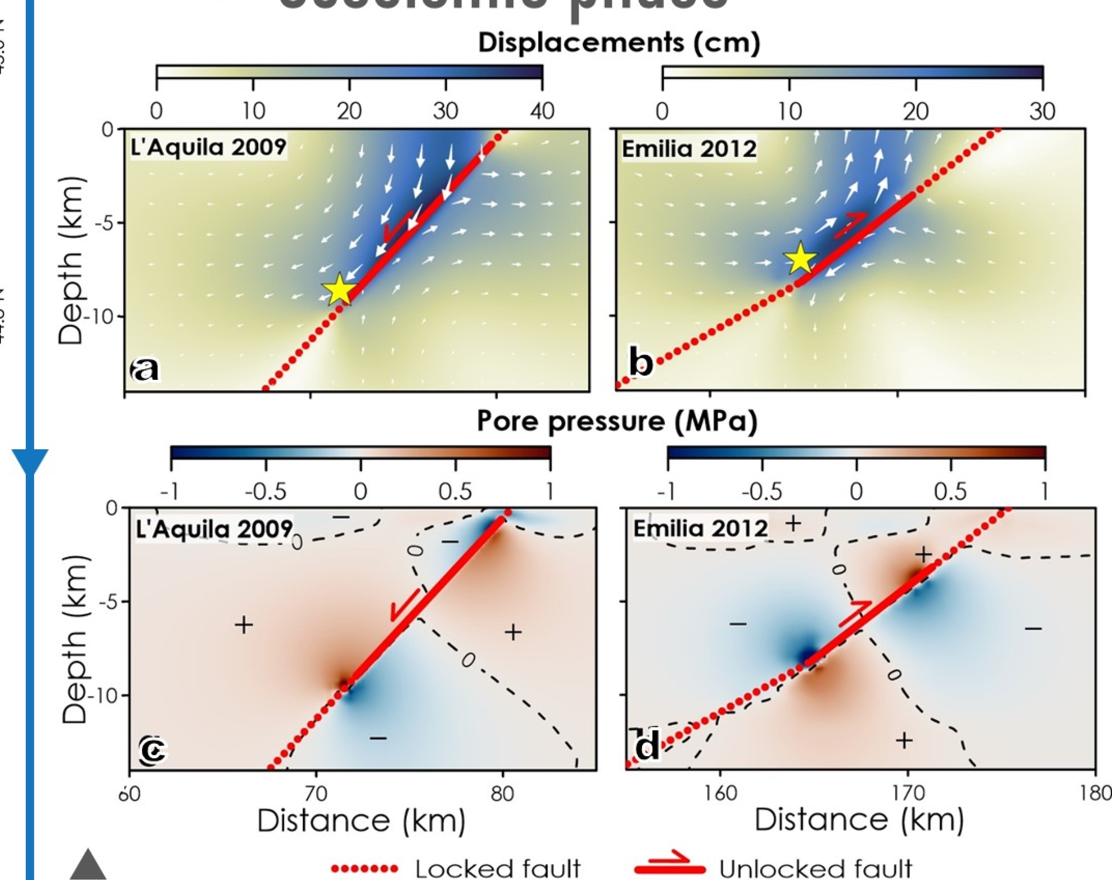

Fig. 7. The coseismic dislocation of the upper fault segment (n°2 in Fig. 4) produces the coseismic displacement fields in panels a and b for the L'Aquila 2009 and Emilia 2012 earthquakes, respectively. These are consistent with the faulting style and magnitude. Since the model is fully-saturated, the instantaneous fault dislocation develops excess pore pressures respect to the hydrostatic values (panels c and d).

Fig. 8. Comparison between the observed (Fig. 2) and modelled (Fig. 7) coseismic displacements along the sections A-A' and B-B' (Fig. 1a) for the L'Aquila 2009 and Emilia 2012 earthquakes, respectively. The modelled displacements along the ascending and descending line of sight are consistent with those observed with satellite data, being the RMSE values comparable with those obtained with kinematic models.

- **Section A-A' (Figure 1a): L'Aquila 2009 earthquake**

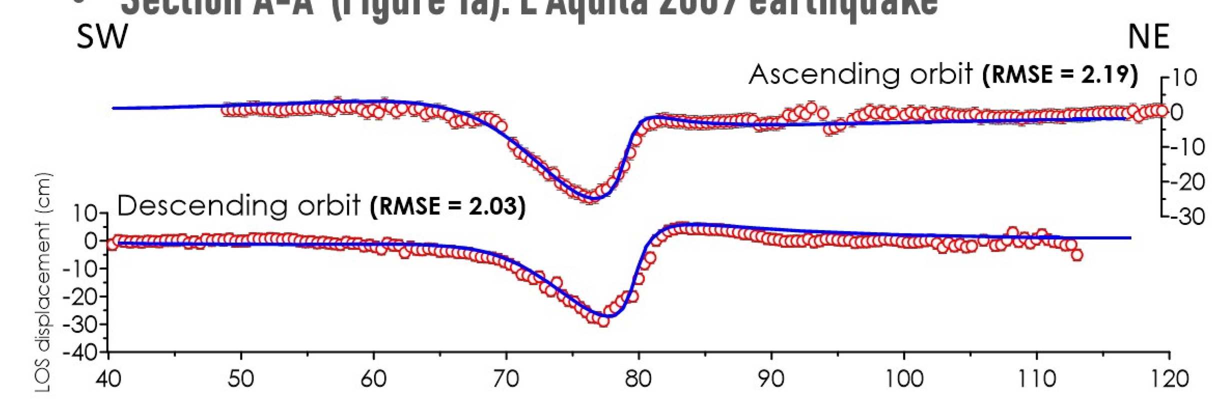

- **Section B-B' (Figure 1a): Emilia 2012 earthquake**

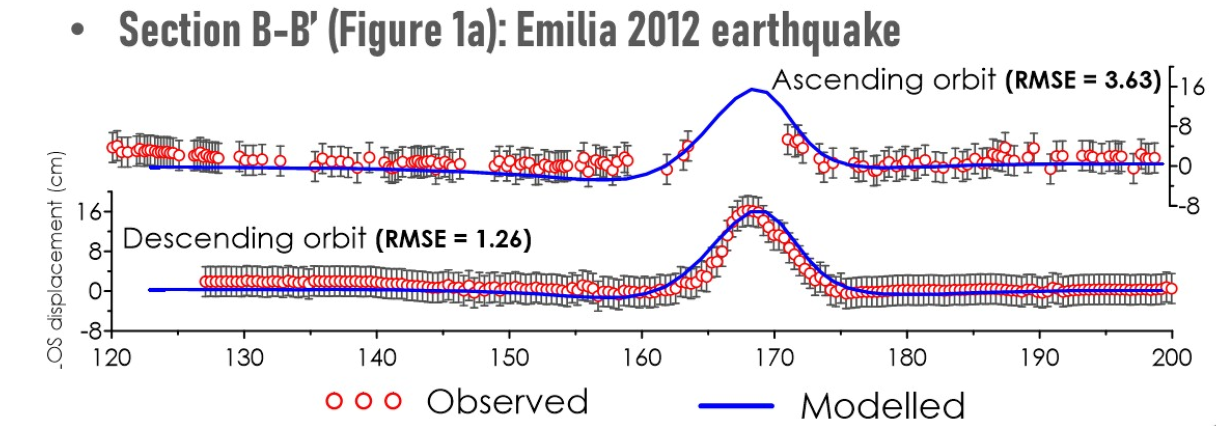

Postseismic phase

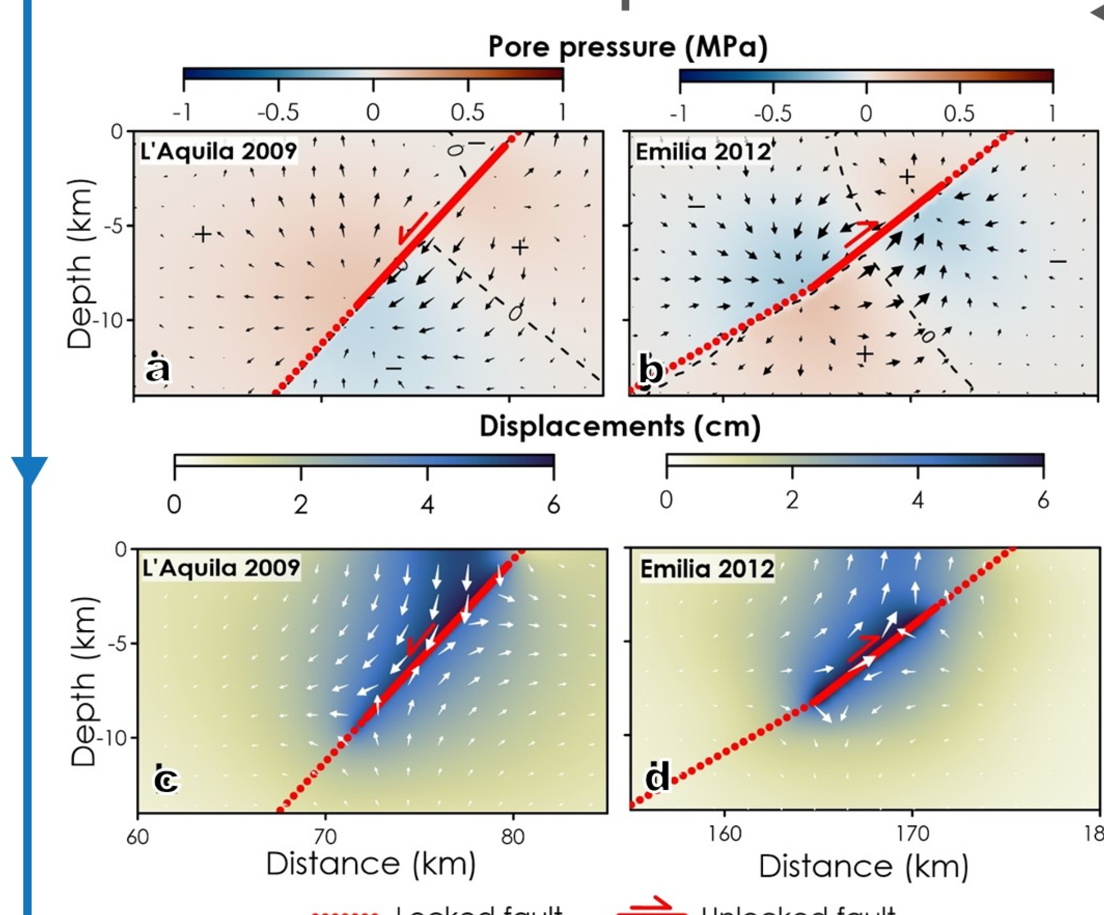

Fig. 8. The coseismic pore pressure excess (Fig. 7 c and d) dissipate in the two-year-long postseismic phase because of fluid diffusion (panel a and b) from suprahydrostatic areas to subhydrostatic areas. Postseismic pore pressure changes modify the effective stresses and strains, thus producing further subsidence of the hanging wall for the L'Aquila 2009 earthquake (panel c) and further uplift of the hanging wall for the Emilia 2012 event (panel (d).

CONCLUSIONS

- The stress gradient generated at the brittle-plastic transition during the interseismic phase yields dilation at the base of a locked normal fault, with the formation of cracks and porosity increase, and contraction at the base of a locked thrust fault, with crack closure and porosity decrease.
- This partitioning of the interseismic stress and strain at the transition between the brittle and plastic fault segments promotes the coseismic subsidence and uplift of the hanging wall in extensional and compressional regimes, respectively.
- The observed postseismic relaxation (where the model is driven by poroelasticity) shows further ground subsidence and uplift for normal and reverse faulting earthquakes, respectively, in agreement with the faulting style.

References:

- Carminati, E., Doglioni, C., 2012. Alps vs. Apennines: The paradigm of a tectonically asymmetric Earth. Earth-Science Rev. 112, 67–96. https://doi.org/10.1016/J.EARSCIREV.2012.02.004
- Doglioni, C., Barba, S., Carminati, E., Riguzzi, F., 2011. Role of the brittle-ductile transition on fault activation. Phys. Earth Planet. Inter. 184, 160–171. https://doi.org/10.1016/j.pepi.2010.11.005
- Crameri, F., 2018. Scientific colour-maps. https://doi.org/10.5281/ZENODO.1287763